Estimating Tropical Cyclone Central Pressure and Outer Winds from Satellite Microwave Data

STANLEY Q. KIDDER, WILLIAM M. GRAY AND THOMAS H. VONDER HAAR

Department of Atmospheric Science, Colorado State University, Fort Collins 80523

(Manuscript received 24 April 1978, in final form 10 July 1978)

ABSTRACT

A technique is proposed for estimating tropical cyclone central pressure and surface wind speeds outside of the radius of maximum wind speed from the 55.45 GHz channel of the Scanning Microwave Spectrometer on board the Nimbus 6 satellite. The method was developed using measurements over eight typhoons and five hurricanes during 1975.

1. Introduction

Since the launch of the first meteorological satellites, scientists have been using the data to obtain information about tropical cyclones (Sadler, 1964). The attempts to measure surface wind speeds and central pressures have centered on the identification in visible-light satellite images of certain cloud features such as the nature and amount of banding, the shape of the cirrus overcast and the appearance of the eye (Fett, 1966; Fritz *et al.*, 1966, Shenk and Salomonson, 1970). The technique has evolved until today the scheme of Dvorak (1975) is widely used (Gaby *et al.*, 1977) to estimate storm intensity (maximum sustained surface wind speed) and central pressure (minimum sea level pressure). Very little work has been done on estimating surface wind speeds at outer radii from satellite data. Recently, new satellite data have become available which promise to improve wind and pressure estimates.

With the launch of the Nimbus 5 and Nimbus 6 satellites in 1972 and 1975, respectively, scanning radiometer data have become available in the radio window of the earth's atmosphere (1 mm to a few meters).[1] Some of the atmospheric and surface parameters to which microwave radiation is sensitive are atmospheric temperature, moisture and liquid water content, precipitation, surface temperature, soil moisture content and ocean foam coverage caused by surface winds. [See Wilheit (1972) for a short review of these interactions.] Because clouds are nearly transparent to microwave radiation, these parameters are observable even in overcast situations. It is not surprising, therefore, that many studies of the microwave characteristics of tropical cyclones have begun to appear in the literature (e.g., Allison *et al.*, 1974; Adler and Rodgers, 1976; Rosenkranz *et al.*, 1978). In this paper we will present a new technique for estimating central pressure and surface winds outside of the radius of maximum winds from brightness temperatures measured by the Scanning Microwave Spectrometer on Nimbus 6. We will not treat the problem of estimating maximum surface winds because the spatial resolution of the radiometer is not high enough for this purpose.

2. The radiometer

The Scanning Microwave Spectrometer is a five-channel instrument sensing radiation nominally at 22.235, 31.65, 52.85, 53.85 and 55.45 GHz (Staelin *et al.*, 1975). The upper three channels are used for sounding the atmosphere, while the lower two are used to measure integrated atmospheric water vapor and liquid water content. The lower two have also been used to measure surface wind speed in Typhoon June (Rosenkranz *et al.*, 1978). The radiometer scans across the spacecraft track in 13 steps at 7.2° intervals each 16 s. The half-power beamwidth is 7.5°, which results in a spatial resolution of 145 km at nadir degrading to 220 km downtrack by 360 km crosstrack at the maximum scan angle. The orbit and scan geometries are such that the earth is viewed completely twice per day, and more often near the poles. The data are recorded on magnetic tape and archived at the National Space Science Data Center, Greenbelt, MD.

The upper three channels are located on the wing of an oxygen absorption band. In the absence of

[1] The first earth-looking microwave radiometer in space was on board the Cosmos 243 satellite launched in September 1968 (Basharinov *et al.*, 1971). It did not scan, however, and thus had limited usefulness in tropical cyclone research.

0027-0644/78/1458-1464$05.00

scattering (due to particles of diameter ≥ 0.2 mm; i.e., precipitation) the brightness temperature observed by channel i ($i = 3, 4, 5$) of the radiometer is given by

$$T_{B_i} = \epsilon_i T_s t_i + \int_0^\infty T(z) W_i(z) dz,$$

where ϵ_i is the surface emissivity, t_i the transmittance from the surface to the satellite, T_s the surface temperature, $T(z)$ the atmospheric temperature at height z and $W_i(z)$ a weighting function (Staelin *et al.*, 1975). $W_i(z)$ is weakly dependent on temperature, humidity and ϵ_i, and is more strongly dependent on scan angle. Fig. 1 shows the SCAMS weighting functions suitable for use over an ocean surface, where $\epsilon_i \leq 0.5$.

The rms noise levels of the radiometer are 0.2 K for the lower two channels and 0.5 K for the upper three. The absolute accuracy is ± 1.5 K (Rosenkranz *et al.*, 1978).

3. Temperature anomalies

The strong surface winds in a tropical cyclone can be traced through the hydrostatic and gradient wind equations to temperature anomalies centered in the upper troposphere. Frank (1977) has calculated the azimuthally-averaged temperature anomaly (difference from temperatures 14° from the storm center) for the mean typhoon (Fig. 2). The main feature is the large positive anomaly centered between 250 and 300 mb and extending several hundred kilometers from the center of the storm. A much smaller cold anomaly exists at approximately 100 mb. Atlantic storms exhibit a very similar structure (LaSeur and Hawkins, 1963; Hawkins and Rubsam, 1968; Hawkins and Imbembo, 1976; Gray, 1977).

Because the weighting function for SCAMS channel 5 peaks in the region of maximum temperature anomaly, one would expect to see a positive anomaly in the channel 5 brightness temperature over tropical cyclones. Indeed, these anomalies have been observed previously by Rosenkranz and Staelin (1976) and by Rosenkranz *et al.* (1978) for west Pacific Typhoon June of 1975. In an effort to substantiate the above findings and to relate them to surface characteristics of the storms, we obtained SCAMS data for eight typhoons and five hurricanes during 1975 (Table 1). In all, 116 microwave images of the storms were collected. The quality of the images varies according to the minimum distance of the subsatellite point from the center of the storm and the amount of missing data. The storms were positioned by interpolating between 6 h best

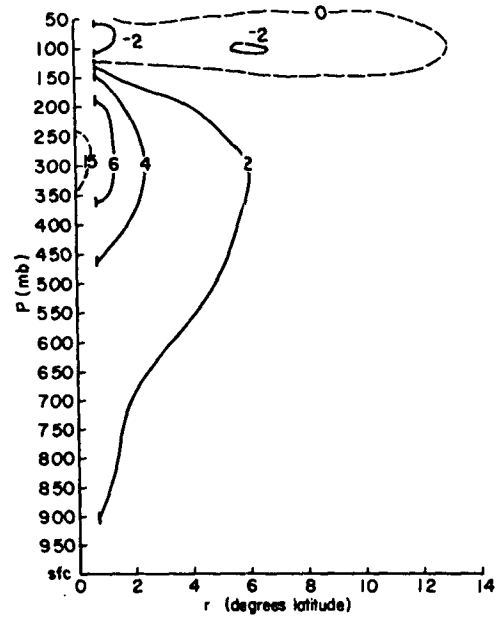

FIG. 2. Temperature anomalies for the mean typhoon (after Frank, 1977).

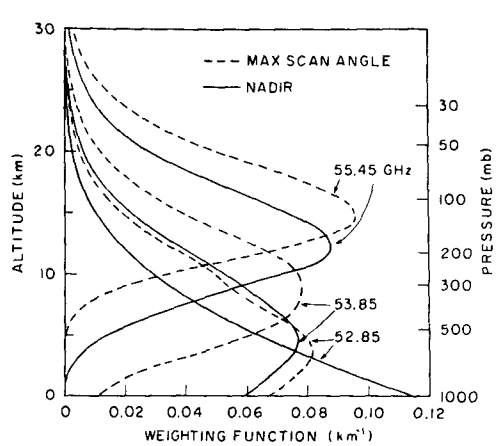

FIG. 1. SCAMS weighting functions for use over an oceanic surface (after Staelin *et al.*, 1975).

TABLE 1. Tropical cyclones used in this study (all 1975).

Name	Peak intensity (kt)	Date/time (GMT) of peak intensity	Minimum sea level pressure (mb)	Central location at time of peak intensity
June	160	19 Nov/12	875	13.2°N, 141.0°E
Phyllis	120	14 Aug/18	925	24.1°N, 137.1°E
Rita	80	22 Aug/12	—	32.9°N, 134.4°E
Tess	95	4 Sep/18	945	23.0°N, 147.6°E
Winnie	65	10 Sep/06	—	31.0°N, 162.8°E
Alice	75	17 Sep/12	973	15.4°N, 123.1°E
Betty	95	22 Sep/00	947	22.6°N, 123.6°E
Cora	105	4 Oct/18	943	30.3°N, 133.2°E
Caroline	100	31 Aug/00	963	24.0°N, 97.0°W
Doris	95	2 Sep/18	—	37.7°N, 44.2°W
Eloise	110	23 Sep/06	961	28.4°N, 87.3°W
Faye	84	26 Sep/18	979	31.0°N, 63.1°W
Gladys	125	2 Oct/00	942	31.0°N, 73.0°W

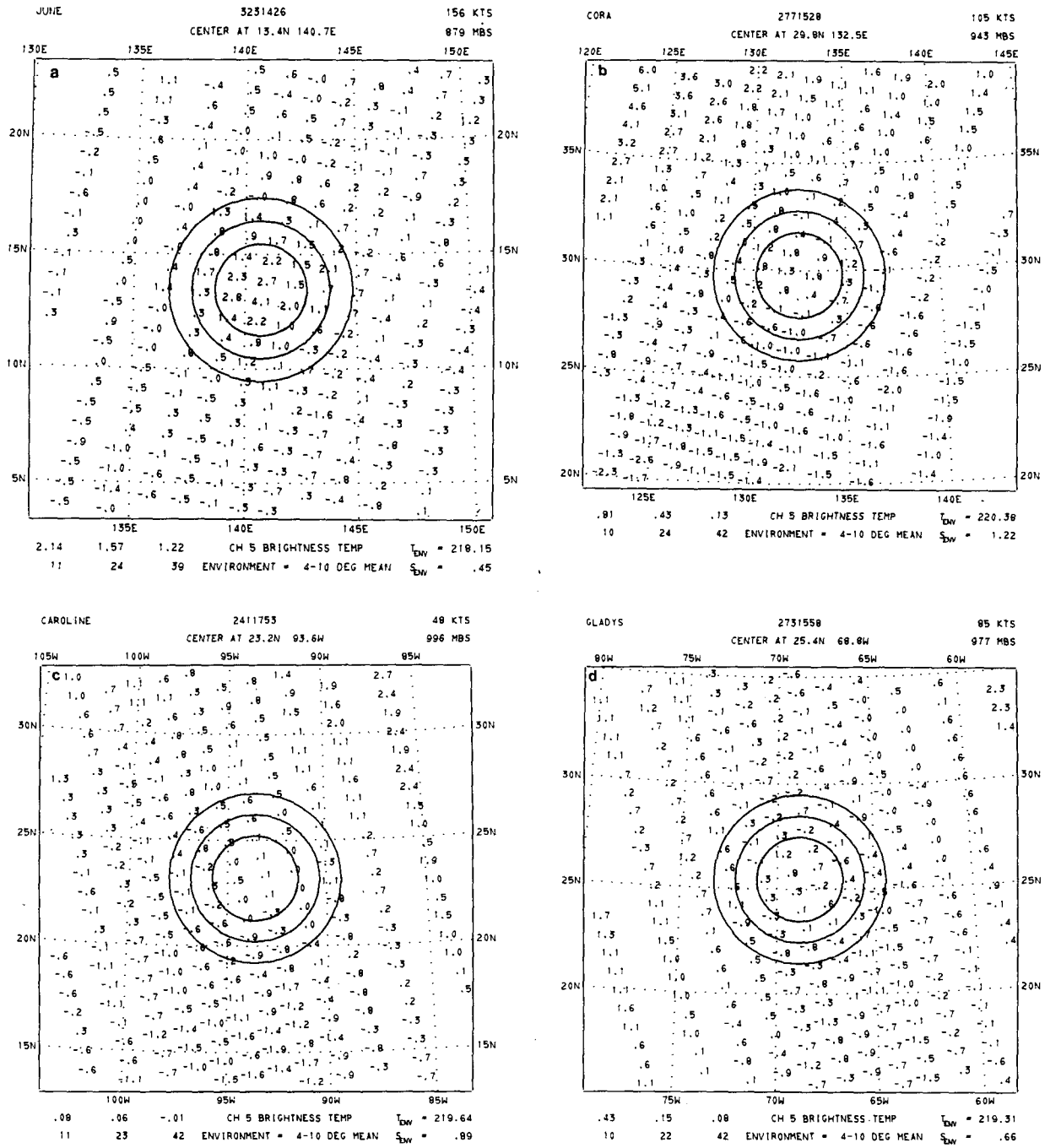

FIG. 3. 55.45 GHz brightness temperature anomalies (K). The three circles are at radii of 2°, 3° and 4° latitude from the interpolated best track storm center. The interpolated wind speed and central pressure are shown in the upper right-hand corner. The environmental mean brightness temperature and its standard deviation are shown in the bottom right-hand corner. The numbers in the bottom left-hand corner are the mean anomalies inside the 2°, 3° and 4° circles and the number of points used to calculate the means. (a) Typhoon June on 19 November 1975 at 1426 GMT; (b) Typhoon Cora on 4 October 1975 at 1528 GMT; (c) Hurricane Caroline on 29 August 1975 at 1753 GMT; (d) Hurricane Gladys on 30 September 1975 at 1558 GMT.

track locations obtained from the *1975 Annual Typhoon Report* and from Hebert *et al.* (1977). Maximum sustained surface wind speed estimates for the typhoons were interpolated from the best track estimates from the *Typhoon Report*. Hurricane winds were interpolated between aircraft measurements, when available, and between satellite estimates, otherwise, both from Hebert *et al.* (1977). [These satellite estimates did not make use of microwave data; they are based on cloudiness

images using primarily the technique of Dvorak (1975).] Central pressure estimates were interpolated between aircraft observations in Hebert *et al.* (1977) and Staff, JTWC (1976).

Fig. 3 shows examples of channel 5 brightness temperature anomalies over four storms of varying intensity. The temperatures plotted are the difference between the observed brightness temperatures and the mean brightness temperature in the region between 4° and 10° latitude from the storm center (the environment). Before the environmental temperature was calculated, all temperatures were corrected for scan angle by adding the temperatures listed in Table 2. This correction was developed by Rosenkranz *et al.* (1978) to account for slight limb darkening due to the increase in height of the weighting function peak with scan angle (see Fig. 1).

Surface winds greater than 7 m s^{-1} cause sea foam formation which increases surface emissivity and can increase satellite observed brightness temperatures (Nordberg *et al.*, 1971). However, the SCAMS channel 5 weighting function is zero at the surface; thus, the channel 5 brightness temperatures are not affected by surface winds. Clouds and precipitation also alter the satellite-observed brightness temperature. At the levels sensed by SCAMS channel 5, most of the cloud droplets will be frozen (air temperature ≤ -20°C) which reduces their microwave absorption about two orders of magnitude (Westwater, 1972). Most of the precipitation is far below the peak of the channel 5 weighting function and should thus only change the satellite-observed brightness temperature slightly, and, because of backscattering by the raindrop-size particles, heavy rain will *decrease* the brightness temperature (Tsang *et al.*, 1977). We conclude that the brightness temperature anomalies plotted in Fig. 3 represent real atmospheric temperature anomalies. This same conclusion was reached by Rosenkranz *et al.* (1978).

Typhoon June (Fig. 3a) was an extremely large storm with 50 kt winds extending 200 n mi from the center (*1975 Annual Typhoon Report*). The warming in the center of June is striking. It extends 3° from the center and reaches 4.1 K. The warming in less intense storms is of lower magnitude and covers a smaller area. In weak storms such as Caroline, however, the warming is probably within the noise level of the data. Thus, it seems that the first experimental microwave sounders demonstrate a definite capability to detect the variation of temperature anomaly in the upper core of the stronger tropical cyclones.

TABLE 2. Corrections to channel 5 (55.45 GHz) for scan angle away from vertical.

Scan angle (deg)	Correction (K)
7.2	0.1
14.4	0.6
21.6	1.8
28.8	3.2
36.0	4.9
43.2	7.2

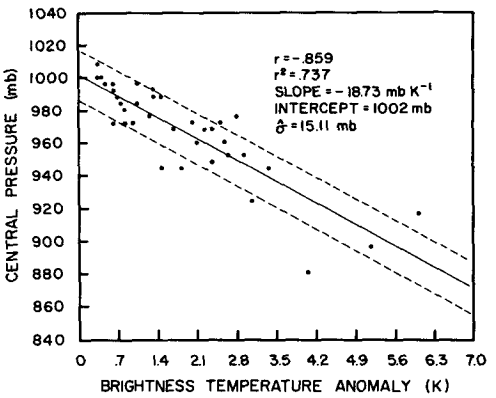

FIG. 4. Central pressure versus maximum channel 5 brightness temperature anomaly within 2° latitude of the interpolated best track center.

4. Central pressures

The central pressure drop in a tropical cyclone is directly the result of *upper tropospheric* warming and the observed fact that the height of the 50 mb level is virtually undisturbed by the tropical cyclone below it (Frank, 1977). If one knows the temperature of the atmosphere and the height of the 50 mb surface, one can calculate the surface pressure with the hydrostatic equation. Because the SCAMS channel 5 brightness temperature is proportional to a weighted mean upper tropospheric temperature, it ought to be correlated with surface pressure. [See Gray (1977) for elaboration of this point.] However, the height (with respect to pressure) of the tropopause decreases from equator to pole and the temperature of the lower stratosphere increases. Since the peak of the SCAMS channel 5 weighting function is at a constant pressure, the environmental brightness temperature increases away from the equator. This is clearly evident in Fig. 3b. To avoid latitude corrections, we correlated central pressure with brightness temperature *anomalies* rather than with the brightness temperature itself. This is equivalent to assuming that the tropical environment around the storm has a constant pressure.

A plot of central pressure versus maximum channel 5 brightness temperature anomaly within 2° of the storm center for the cases (a) for which we had central pressure estimates, and (b) in which the satellite viewing angle was less than or equal to 28.8°, is shown in Fig. 4. Of the 36 data points, 9 are from hurricanes and 27 from typhoons. The

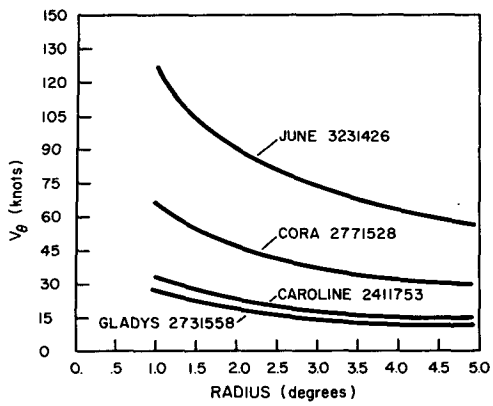

FIG. 5. Calculated tangential winds for the four storms in Fig. 3.

correlation coefficient is −0.859, and the best estimate of the standard deviation from the regression line is ±15 mb. There is a regrettable lack of data at lower surface pressures, but the expected decrease in surface pressure with increasing 55.45 GHz brightness temperature appears to be established. Before this technique can be of operational use, however, more data need to be examined and a more precise brightness temperature-surface pressure relationship derived.

Some causes of variance in Fig. 4 are as follows:

1) Radiometer noise.
2) Warm core region smaller than radiometer resolution and of variable size.
3) Non-constant environmental pressure.
4) Vertical variation of the position of maximum warming.
5) The scan-angle correction.
6) Non-centering of the warm core region in the radiometer scan spot.
7) Weighting function peak not at level of maximum temperature anomaly.
8) Clouds and precipitation.

Particularly serious is the mismatch between size of the eye and radiometer resolution. The three lowest pressure points in Fig. 4 are all from Typhoon June. The left-most point (19 November 1426 GMT) is near the time of peak intensity. The two points to the right (0213 GMT 20 November and 1445 GMT 21 November, respectively) represent the decaying stage. During this time period (19–21 November) the eye changed from a circle with a 5 n mi diameter to a 25 by 40 n mi ellipse (Staff, JTWC, 1976). This problem points out the need for better resolution of future radiometers. Some of the other sources of variance (3,5,8) may be corrected by more rigorous treatment of the data, and some (1,7) could be alleviated in the future by different radiometer design and/or orbit geometry. It is encouraging, however, that this preliminary treatment of the data yields such a high correlation between central surface pressure and brightness temperature anomaly of the storms.

5. Outer winds

The winds in a tropical cyclone are caused by large horizontal pressure gradients. If one has an estimate of the pressure field, one can obtain an estimate of the wind field. Because the 145 km resolution of SCAMS is too coarse to resolve the region of maximum winds, we confined ourselves to estimating winds outside of the radius of maximum winds. This information is important for ship operations and for estimating damage should the storm strike land. We used the regression line in Fig. 4 to estimate the surface pressure field from the SCAMS channel 5 brightness temperature anomalies, and we calculated the azimuthally-averaged tangential surface winds as follows. It has been suggested by Hughes (1952), Riehl (1954, 1963) and Shea (1972) that outside the radius of maximum wind, the tangential wind varies with radius as

$$V_\theta = Cr^{-x}, \tag{2}$$

where x is approximately 0.5. We assumed that $x = 0.5$ and that the tangential winds were in gradient balance, with the radius of curvature of the trajectories equal to the distance from the center of the storm, i.e.,

$$RT\frac{\partial(\ln p)}{\partial r} = \frac{V_\theta^2}{r} + fV_\theta, \tag{3}$$

where R is the gas constant, T the atmospheric temperature and f the Coriolis parameter. Treating f and T as constants, Eq. (3) can be integrated to give

$$\ln(p/p_0) = (1/RT)[-(C^2/r) + 2fCr^{1/2}], \tag{4}$$

where p_0 is an integration constant. Setting

$$y = RT\ln p, \tag{5}$$

where p is the observed surface pressure, we find by the method of least squares that C is the positive, real root of

$$\begin{aligned}[(\Sigma r^{-2}) - N^{-1}(\Sigma r^{-1})^2]C^3 \\ + 3f[N^{-1}(\Sigma r^{-1})(\Sigma r^{1/2}) - (\Sigma r^{-1/2})]C^2 \\ + \{(\Sigma y r^{-1}) - N^{-1}(\Sigma y)(\Sigma r^{-1}) \\ + 2f^2[(\Sigma r) - N^{-1}(\Sigma r^{1/2})^2]\}C \\ + f[N^{-1}(\Sigma y)(\Sigma r^{1/2}) - (\Sigma y r^{1/2})] = 0.\end{aligned} \tag{6}$$

Although the regression line in Fig. 4 underestimates pressures (being based on observations of a relatively small warm core region), and although there is noise in the pressure field produced, we believe that the azimuthal averaging inherent in the least-squares

technique produces approximately the correctly radial pressure gradients and azimuthally-averaged tangential winds at large radii. For $T = 300$ K, we calculated tangential winds using the position of the maximum temperature anomaly inside the 2° radius as the center of the storm. Fig. 5 shows the results for the four storms in Fig. 3. Note the large differences in the outer circulations. We have as yet no actual surface wind data with which to compare these curves. They appear to be reasonable, yet the winds for Gladys seem to be underestimated, and, in a few cases not shown, the winds at 1° radius are larger than the interpolated maximum winds.

This treatment of the problem is, of course, only a first approach to the inference of wind speed. Tropical storms are notoriously asymmetric. Some of the asymmetries could be included by adding the storm motion to the calculated winds, and by calculating tangential winds in various quadrants. We believe that these corrections plus a more sophisticated treatment of the brightness temperature-wind relationship could yield a good estimate of the wind field around tropical cyclones.

6. Summary and conclusions

In this paper we have shown that the warm 55.45 GHz brightness temperature anomaly previously observed over Typhoon June can be found over other tropical cyclones. Physical considerations led us to examine such upper tropospheric measurements as a potential indicator of the storm's surface pressure pattern. We have correlated maximum brightness temperature anomaly with central pressure and calculated a correlation coefficient of −0.859. Finally, we calculated outer surface wind speeds by assuming gradient balance and using the regression between brightness temperature anomaly and central pressure to estimate pressure gradients. These winds appear to be reasonable, but they have not been verified against observations.

In this time of increasing expense and decreasing frequency of aircraft reconnaisance of tropical cyclones, satellite observations are becoming more and more important. We believe that the technique of using SCAMS-type data for measuring surface winds and pressures in tropical cyclones appears very promising and deserves further attention. Our methods should be explored in connection with the other new methods becoming available. Microwave radiometers soon to be flown on the TIROS-N and DMSP satellites will provide additional data to test this technique, and Spacelab will provide the opportunity for further refinement.

Acknowledgments. The authors would like to thank Drs. D. H. Staelin and P. W. Rosenkranz of MIT for their encouragement and help in the interpretation of the data tapes, Dr. W. M. Frank of CSU for helpful discussions, and Ms. Donna Willey and Janice P. Root for typing the manuscript. This research was sponsored in part by NASA under Grants NGR-06-002-102 and NSG-5258 and by Colorado State University.

REFERENCES

Adler, R. F., and E. B. Rodgers, 1977: Satellite-observed latent heat release in a tropical cyclone. *Mon. Wea. Rev.*, **105**, 956–963.

Allison, L. J., E. B. Rodgers, T. T. Wilheit and R. W. Fett, 1974: Tropical cyclone rainfall as measured by the Nimbus 5 electrically scanning microwave radiometer. *Bull. Amer. Meteor. Soc.*, **55**, 1074–1089.

Basharinov, A. E., S. T. Yegorov, A. S. Gurvich, and A. M. Oboukhov, 1971: Some results of microwave sounding of the atmosphere and ocean from the satellite Cosmos 243. Space Research XI, COSPAR, Berlin, 593–600.

Dvorak, V. F., 1975: Tropical cyclone intensity analysis and forecasting from satellite imagery. *Mon. Wea. Rev.*, **103**, 420–430.

Fett, R. W., 1966: Upper-level structure of the formative tropical cyclone. *Mon. Wea. Rev.*, **94**, 9–18.

Frank, W. M., 1977: The structure and energetics of the tropical cyclone I. Storm structure. *Mon. Wea. Rev.*, **105**, 1119–1135.

Fritz, S., L. F. Hubert and A. Timchalk, 1966: Some inferences from satellite pictures of tropical disturbances. *Mon. Wea. Rev.*, **94**, 231–236.

Gaby, D. C., J. B. Lushine, B. M. Mayfield, S. C. Pearce, K. O. Poteat, and F. E. Torres, 1977: Atlantic tropical and subtropical cyclone classifications for 1976. NOAA Tech. Memor. NESS 87, 13 pp. [NTIS PB 269 674/8GI].

Gray, W. M., 1977: Cyclone intensity determination through upper tropospheric reconnaissance. *Postprints 11th Tech. Conf. Hurricanes and Tropical Meteorology*, Miami, 288–293.

Hawkins, H. F., and D. T. Rubsam, 1968: Hurricane Hilda, 1964 II. Structure and budgets of the hurricane on October 1, 1964. *Mon. Wea. Rev.*, **96**, 617–636.

——, and S. M. Imbembo, 1976: The structure of a small intense hurricane—Inez, 1966. *Mon. Wea. Rev.*, **104**, 418–442.

Hebert, P. J., and Staff, NHC, 1977: Annual data and verification tabulation Atlantic tropical cyclones 1975. NOAA Tech. Memo. NWS NHC 2, Miami, 63 pp.

Hughes, L. A., 1952: On the low level wind structure of tropical cyclones. *J. Meteor.*, **9**, 422–428.

LaSeur, N. E., and H. F. Hawkins, 1963: An analysis of hurricane Cleo (1958) based on data from research reconnaissance aircraft. *Mon. Wea. Rev.*, **91**, 694–709.

Nordberg, W., J. Conaway, D. B. Ross and T. Wilheit, 1971: Measurements of microwave emission from a foam-covered, wind-driven sea. *J. Atmos. Sci.*, **28**, 429–435.

Riehl, H., 1954: *Tropical Meteorology*. McGraw-Hill, 392 pp.

——, 1963: Some relations between wind and thermal structure of steady-state hurricanes. *J. Atmos. Sci.*, **20**, 276–287.

Rosenkranz, P. W., and D. H. Staelin, 1976: Summary of operations: The scanning microwave spectrometer (SCAMS) experiment. *The Nimbus 6 Data Catalog*, Vol. 3, NASA/Goddard Space Flight Center, Greenbelt, MD, 2–6 pp.

——, —— and N. C. Grody, 1978: Typhoon June (1975) viewed by a scanning microwave spectrometer. *J. Geophys. Res.*, **83**, 1857–1868.

Sadler, J. C., 1964: Tropical cyclones of the Eastern North Pacific as revealed by TIROS observations. *J. Appl. Meteor.*, **3**, 347–366.

Shea, D. J., 1972: The structure and dynamics of the hurricane's

inner core region. Atmos. Sci. Pap. 182, Colorado State University, Fort Collins, 134 pp.

Shenk, W. E., and V. V. Salomonson, 1970: Visible and infrared imagery from meteorological satellites. *Appl. Opt.*, **9**, 1747–1769.

Staelin, D. H., A. H. Barrett, P. W. Rosenkranz, F. T. Barath, E. J. Johnson, J. W. Waters, A. Wouters and W. B. Lenoir, 1975: The scanning microwave spectrometer (SCAMS) experiment. *The Nimbus 6 User's Guide*, J. E. Sissala, Ed., LANDSAT/Nimbus Project, NASA/Goddard Space Flight Center, Greenbelt, MD, 59–86 pp.

Staff, Joint Typhoon Warning Center, 1975: *1975 Annual Typhoon Report*. Joint Typhoon Warning Center, COMNAVMARIANAS Box 12, FPO, San Francisco.

——, 1976: Tropical cyclone center fix data for the 1975 typhoon season. FLEWEACEN Tech. Note JTWC 76-5, Joint Typhoon Warning Center, COMNAVMARIANAS Box 12, FPO, San Francisco, 35 pp.

Tsang, L., J. A. Kong, E. Njoku, D. H. Staelin and J. W. Waters, 1977: Theory for microwave thermal emission from a layer of cloud or rain. *IEEE Trans. Antennas Propagation*, **AP-24**, 650–657.

Westwater, E. R., 1972: Microwave emission from clouds. NOAA Tech. Rep. 219-WPL 18, Boulder, 43 pp.

Wilheit, T. T., 1972: The electrically scanning microwave radiometer (ESMR) experiment. *The Nimbus 5 User's Guide*, R. R. Sabatini, Ed., ERTS/Nimbus Project, NASA/Goddard Space Flight Center, Greenbelt, MD, 59–105.